IEICE TRANS. FUNDAMENTALS, VOL.E94–A, NO.10 OCTOBER 2011

PAPER

Two Dimensional Non-separable Adaptive Directional Lifting Structure of Discrete Wavelet Transform

Taichi YOSHIDA[†a)], ***Student Member***, **Taizo SUZUKI**[††], **Seisuke KYOCHI**[†], ***and*** **Masaaki IKEHARA**[†], ***Members***

SUMMARY In this paper, we propose a two dimensional (2D) non-separable adaptive directional lifting (ADL) structure for discrete wavelet transform (DWT) and its image coding application. Although a 2D non-separable lifting structure of 9/7 DWT has been proposed by interchanging some lifting, we generalize a polyphase representation of 2D non-separable lifting structure of DWT. Furthermore, by introducing the adaptive directional filteringingto the generalized structure, the 2D non-separable ADL structure is realized and applied into image coding. Our proposed method is simpler than the 1D ADL, and can select the different transforming direction with 1D ADL. Through the simulations, the proposed method is shown to be efficient for the lossy and lossless image coding performance.

key words: *two dimensional non-separable lifting structure, discrete wavelet transform, adaptive directional filtering, lossy and lossless image coding*

1. Introduction

The discrete wavelet transform (DWT) has been a fundamental tool for image and video processing for the last few decades. It is applied to image coding standard, JPEG 2000 [1], and high quality digital cinema [2]. Despite its success, DWT has a serious disadvantage. Since they can only transform images along the vertical and horizontal directions by separable implementation, they fail to provide sparse representation of transforming images which consist of various angles of directionally-oriented textures except vertical and horizontal directions. Therefore, if DWT is applied to images which contain a rich directional high frequency component, such as edges and contours, the coding efficiency is severely degraded.

To avoid this degradation, an adaptive directional filtering based on a lifting structure has been proposed [3]–[9]. The adaptive directional filtering can flexibly switch the filtering direction according to the direction of edges and contours, and compression efficiency can be improved. Especially, an one dimensional (1D) adaptive directional lifting (ADL) based wavelet transform [5] achieves high compression efficiency for the lossy image coding. However, since 1D ADL has to be separately applied twice for two dimensional (2D) signals, it is redundant and produces a distortion of desired filtering directions due to the down-sampling between the vertical and horizontal filtering. In this paper, hence, we propose the 2D direct and adaptive directional filtering based on DWT, called a 2D non-separable ADL structure of DWT.

The proposed structure is realized by introducing an adaptive directional filtering framework into a 2D direct lifting structure based on DWT. The lifting structure of DWT has been proposed for the integer-to-integer transform [10]. For 2D signals such as images, a 2D separable lifting structure of DWT is realized by applying the 1D lifting structure to images twice, vertically and horizontally. Iwahashi et al. have proposed the 2D direct lifting structure based on 9/7 DWT, by interchanging and merging some lifting in the 2D separable lifting structure of 9/7 DWT [11], [12]. The new structure is called a 2D non-separable lifting structure of 9/7 DWT. The non-separable structure requires less rounding operators than the separable one, and is suitable for the lossless image coding application. In this paper, we generalize the polyphase representation of 2D non-separable lifting structure based on 2-channel 1D filter banks (FBs) such as DWT. It contains the class of the 2D non-separable lifting structure of 9/7 DWT [12]. Our proposed structure can design various 2D non-separable lifting structures.

Furthermore, to improve the efficiency of image coding, we develop the generalized polyphase representation for the adaptive directional filtering. Changing the sampling matrix of the proposed structure, we can change the direction of the transform. The proposed adaptive directional filtering is realized by changing the sampling matrix by sub-regions of images, according to feature directions of the sub-regions. With advantages of the 2D non-separable structure and the adaptive directional filtering, the proposed structure improves the performance of the lossy-to-lossless image coding application. The proposed method is simpler than the 1D one and can select the filtering directions which are different from 1D ADL. Finally, lossy and lossless image coding results of the proposed structure are shown to validate the advantage of the proposed structure.

Section 2 summarizes FB and show a polyphase representation of the 2D separable lifting structure and 1D ADL structure of DWT. We propose the generalized polyphase representation of the 2D non-separable lifting structure of DWT in Sect. 3, and its adaptive directional filtering in Sect. 4. Section 5 shows some image coding results and conclusions are presented in Sect. 6.

Notations: Vectors are denoted by boldfaced lowercase characters, whereas matrices are denoted by boldfaced

Manuscript received January 13, 2011.
Manuscript revised May 17, 2011.

[†]The authors are with the Department of Electronics and Electrical Engineering, Keio University, Yokohama-shi, 223-8522 Japan.
[††]The author is with the College of Engineering, Nihon University, Koriyama-shi, 963-8642 Japan.
a) E-mail: yoshida@tkhm.elec.keio.ac.jp

DOI: 10.1587/transfun.E94.A.1920

uppercase characters. $\mathbf{A}^T$ and $\mathbf{A}^{-1}$ denote the transpose and the inverse of the matrix $\mathbf{A}$, respectively. $\mathbf{I}$ and $\mathbf{0}$ are identity and the null matrices, respectively. $\mathbf{M}$ is a 2×2 nonsingular integer matrix. An absolute determinant of the factor $\mathbf{M}$ is described as $M = |det(\mathbf{M})|$. $\downarrow \mathbf{M}$ and $\uparrow \mathbf{M}$ also represent the down- and up-samplers of $\mathbf{M}$, respectively. Using vectors $\mathbf{z} = [z_x, z_y]^T$ and $\mathbf{k} = [k_x, k_y]^T$, a multiplication of vectors is defined as $\mathbf{z}^{\mathbf{k}} = z_x^{k_x} z_y^{k_y}$. diag$(\cdot)$ denotes the block diagonal matrix as

$$\mathrm{diag}(\mathbf{A}_0, \mathbf{A}_1, \cdots, \mathbf{A}_n) = \begin{bmatrix} \mathbf{A}_0 & \mathbf{0} & \cdots & \mathbf{0} \\ \mathbf{0} & \mathbf{A}_1 & \cdots & \mathbf{0} \\ \vdots & \vdots & \ddots & \vdots \\ \mathbf{0} & \mathbf{0} & \cdots & \mathbf{A}_n \end{bmatrix}.$$

2. Review

2.1 Polyphase Representation of FB

The 1D maximally decimated FB with M-channel can be also represented by polyphase matrices. $\mathbf{E}(z)$ and $\mathbf{R}(z)$ are the type-I polyphase matrix of the analysis bank and the type-II polyphase matrix of the synthesis bank [13]. These polyphase matrices are related to $H_k(\mathbf{z})$ and $F_k(\mathbf{z})$ $(k = 0, 1, \cdots, M-1)$ which denote analysis filters and synthesis filters as

$$\begin{aligned} \mathbf{H}(z) &= [H_0(z), H_1(z), \cdots, H_{M-1}(z)]^T \\ &= \mathbf{E}(z^M)\mathbf{d}_M(z), \\ \mathbf{F}(z) &= [F_0(z), F_1(z), \cdots, F_{M-1}(z)]^T \\ &= \mathbf{d}_M^T(z^{-1})\mathbf{R}(z^M), \end{aligned} \tag{1}$$

where $\mathbf{d}_M(z) = [1, z^{-1}, z^{-2}, \cdots, z^{-(M-1)}]^T$. If the polyphase matrices satisfy the condition as $\mathbf{E}(z)\mathbf{R}(z) = z^{-n}\mathbf{I}$, the result is said to be the perfect reconstruction, where n is an order of the FB. Hence, the synthesis matrix $\mathbf{R}(z)$ is designed as $z^{-n}\mathbf{E}^{-1}(z^{-1})$. For simplicity, the synthesis bank is omitted in this paper.

In a similar way to 1D FB, the 2D maximally decimated FB with $\mathbf{M}$ is represented by the polyphase matrix as

$$\mathbf{H}(\mathbf{z}) = \mathbf{E}(\mathbf{z}^{\mathbf{M}})\mathbf{d}_{\mathbf{M}}(\mathbf{z}), \tag{2}$$

where $\mathbf{M}$ is referred to as a sampling matrix, $\mathbf{z} = [z_x, z_y]$, z_x and z_y are the vertical and horizontal delay elements, respectively,

$$\begin{aligned} \mathbf{d}_{\mathbf{M}}(\mathbf{z}) &= [\mathbf{z}^{-\mathbf{k}_0}, \mathbf{z}^{-\mathbf{k}_1}, \cdots, \mathbf{z}^{-\mathbf{k}_{M-1}}]^T, \\ \mathbf{z}^{\mathbf{M}} &= [z_0^{m_{0,0}} z_1^{m_{1,0}}, z_0^{m_{0,1}} z_1^{m_{1,1}}]^T, \end{aligned}$$

$\mathbf{k}_i$ is an integer vector of a set $\Xi(\mathbf{M})$, called as a delay vector, $\mathbf{k}_0$ is restricted to be $[0, 0]^T$, $\Xi(\mathbf{M})$ is a set of integer vectors, which is defined as

$$\Xi(\mathbf{M}) = \{\mathbf{M}\mathbf{x} \mid \mathbf{x} \in [0, 1)\},$$

$\mathbf{x} \in [0, 1)$ denotes a set of 2×1 real vectors $\mathbf{x}$ whose the ith component satisfies $0 \le x_i < 1$ and $m_{i,j}$ denotes the (i, j) element of $\mathbf{M}$.

2.2 2D Separable Lifting Structure of DWT

1D DWT is classified into 2-channel FB. Its lifting structure can be expressed in the polyphase representation as follows [10], [13].

$$\begin{aligned} \begin{bmatrix} H_L(z) \\ H_H(z) \end{bmatrix} &= \hat{\mathbf{E}}(z^2)\mathbf{d}_2(z) \\ \hat{\mathbf{E}}(z) &= \begin{bmatrix} s & 0 \\ 0 & 1/s \end{bmatrix} \prod_{i=N-1}^{0} \left\{ \begin{bmatrix} 1 & U_i(z) \\ 0 & 1 \end{bmatrix} \begin{bmatrix} 1 & 0 \\ P_i(z) & 1 \end{bmatrix} \right\} \end{aligned} \tag{3}$$

This structure with $N = 2$ is shown in Fig. 1, where R denotes a rounding operator. This figure shows that 1D signals are divided into even samples and odd samples, sample is transformed with the other sample, and even and odd samples are conclusively output as lowpass and highpass coefficients, respectively. In general, down-arrows from even signals to odd signals are called a prediction step, and up-arrows are called an update step.

The pair of scaling factors can be realized as a lifting structure [10]. The scaling factors are factorized as

$$\begin{bmatrix} s & 0 \\ 0 & 1/s \end{bmatrix} = \begin{bmatrix} 1 & s - s^2 \\ 0 & 1 \end{bmatrix} \begin{bmatrix} 1 & 0 \\ -1/s & 1 \end{bmatrix} \begin{bmatrix} 1 & s-1 \\ 0 & 1 \end{bmatrix} \begin{bmatrix} 1 & 0 \\ 1 & 1 \end{bmatrix}. \tag{4}$$

Figure 2 show the lifting realization of scaling factors, where $s_0 = s - 1$, $s_1 = -1/s$ and $s_2 = s - s^2$. The lifting structure with rounding operators can transform signals from integer to integer. Note that scaling parts can also be constructed by lifting steps.

According to the separable implementation, the 2D separable lifting structure of DWT can be given by

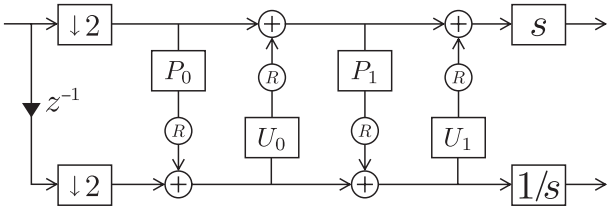

Fig. 1 9/7 DWT.

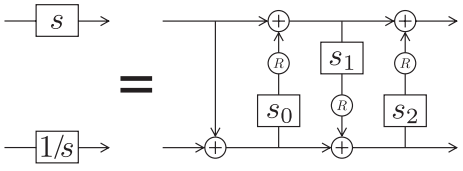

Fig. 2 Lifting realization of scaling.

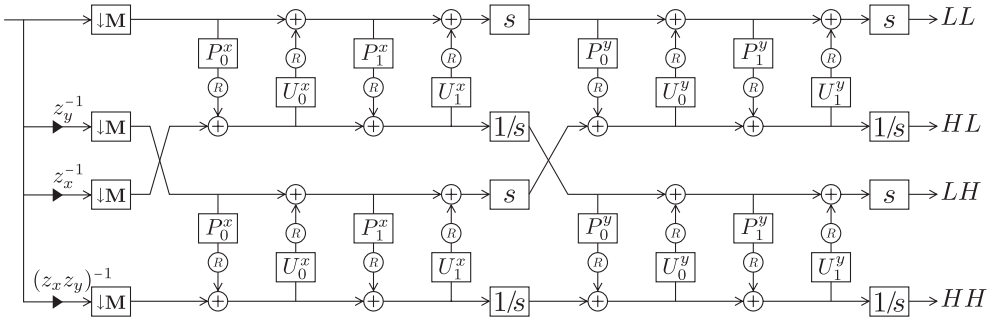

Fig. 3 2D separable lifting structure of 9/7 DWT.

$$\begin{aligned}\mathbf{H}(\mathbf{z}) &= \begin{bmatrix} H_{LL}(\mathbf{z}) \\ H_{HL}(\mathbf{z}) \\ H_{LH}(\mathbf{z}) \\ H_{HH}(\mathbf{z}) \end{bmatrix} = \begin{bmatrix} H_L(z_x)H_L(z_y) \\ H_L(z_x)H_H(z_y) \\ H_H(z_x)H_L(z_y) \\ H_H(z_x)H_H(z_y) \end{bmatrix} \\ &= \begin{bmatrix} H_L(z_y) & 0 \\ H_H(z_y) & 0 \\ 0 & H_L(z_y) \\ 0 & H_H(z_y) \end{bmatrix} \times \begin{bmatrix} H_L(z_x) \\ H_H(z_x) \end{bmatrix} \\ &= \begin{bmatrix} \hat{\mathbf{E}}(z_y^2) & \mathbf{0} \\ \mathbf{0} & \hat{\mathbf{E}}(z_y^2) \end{bmatrix} \begin{bmatrix} \mathbf{d}_2(z_y) & \mathbf{0} \\ \mathbf{0} & \mathbf{d}_2(z_y) \end{bmatrix} \hat{\mathbf{E}}(z_x^2)\mathbf{d}_2(z_x),\end{aligned} \tag{5}$$

for the four subband filters, $H_{LL}(\mathbf{z})$, $H_{HL}(\mathbf{z})$, $H_{LH}(\mathbf{z})$ and $H_{HH}(\mathbf{z})$. To define the polyphase matrix of 2D separable structure, we introduce the relationships as

$$\begin{cases} \hat{\mathbf{d}}_2(z_y) \begin{bmatrix} s & 0 \\ 0 & 1/s \end{bmatrix} = \begin{bmatrix} s\mathbf{I} & \mathbf{0} \\ \mathbf{0} & 1/s\mathbf{I} \end{bmatrix} \hat{\mathbf{d}}_2(z_y), \\ \hat{\mathbf{d}}_2(z_y) \begin{bmatrix} 1 & U_i(z_x^2) \\ 0 & 1 \end{bmatrix} = \begin{bmatrix} \mathbf{I} & U_i(z_x^2)\mathbf{I} \\ \mathbf{0} & \mathbf{I} \end{bmatrix} \hat{\mathbf{d}}_2(z_y), \\ \hat{\mathbf{d}}_2(z_y) \begin{bmatrix} 1 & 0 \\ P_i(z_x^2) & 1 \end{bmatrix} = \begin{bmatrix} \mathbf{I} & \mathbf{0} \\ P_i(z_x^2)\mathbf{I} & \mathbf{I} \end{bmatrix} \hat{\mathbf{d}}_2(z_y), \end{cases} \tag{6}$$

where $\hat{\mathbf{d}}_2(z_y) = \mathrm{diag}(\mathbf{d}_2(z_y), \mathbf{d}_2(z_y))$. From the above relationships (6), (5) is rewritten as

$$\begin{aligned}\mathbf{H}(\mathbf{z}) = &\begin{bmatrix} \hat{\mathbf{E}}(z_y^2) & \mathbf{0} \\ \mathbf{0} & \hat{\mathbf{E}}(z_y^2) \end{bmatrix} \\ &\times \begin{bmatrix} s\mathbf{I} & \mathbf{0} \\ \mathbf{0} & 1/s\,\mathbf{I} \end{bmatrix} \prod_{i=N-1}^{0} \left\{ \begin{bmatrix} \mathbf{I} & U_i(z_x^2)\mathbf{I} \\ \mathbf{0} & \mathbf{I} \end{bmatrix} \begin{bmatrix} \mathbf{I} & \mathbf{0} \\ P_i(z_x^2)\mathbf{I} & \mathbf{I} \end{bmatrix} \right\} \\ &\times \hat{\mathbf{d}}_2(z_y)\mathbf{d}_2(z_x).\end{aligned} \tag{7}$$

Consequently, the polyphase representation of the above 2D separable structure is described as

$$\begin{aligned}\mathbf{H}(\mathbf{z}) &= \mathbf{E}(\mathbf{z}^{\mathbf{M}})\mathbf{d}_{\mathbf{M}}(\mathbf{z}), \\ \mathbf{E}(\mathbf{z}) &= \begin{bmatrix} \hat{\mathbf{E}}^y & \mathbf{0} \\ \mathbf{0} & \hat{\mathbf{E}}^y \end{bmatrix} \begin{bmatrix} s\mathbf{I} & \mathbf{0} \\ \mathbf{0} & 1/s\,\mathbf{I} \end{bmatrix} \prod_{i=N-1}^{0} \left\{ \begin{bmatrix} \mathbf{I} & U_i^x\mathbf{I} \\ \mathbf{0} & \mathbf{I} \end{bmatrix} \begin{bmatrix} \mathbf{I} & \mathbf{0} \\ P_i^x\mathbf{I} & \mathbf{I} \end{bmatrix} \right\}, \\ \mathbf{d}_{\mathbf{M}}(\mathbf{z}) &= [1, z_y^{-1}, z_x^{-1}, z_x^{-1}z_y^{-1}]^T,\end{aligned} \tag{8}$$

where $\hat{\mathbf{E}}^j$, P_i^j and U_i^j (j : x or y) denote $\hat{\mathbf{E}}(z_j)$, $P_i(z_j)$ and $U_i(z_j)$. Since the 2D FB is realized by the separable implementation of 1D FB, the decimation matrix $\mathbf{M}$ should be diag(2, 2). For example, Fig. 3 shows the 2D separable lifting structure of 9/7 DWT. This figure shows that images are divided into four sets and transformed while maintaining integers.

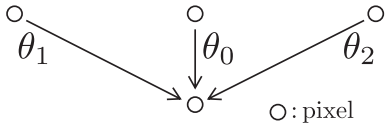

Fig. 4 Lifting direction of 1D ADL.

2.3 1D ADL Structure of DWT

Based on the lifting structure of 1D DWT, 1D ADL is realized by permitting the other directions of the transform except horizontal and vertical [5].

Figure 4 illustrates a 2D signal $x(\mathbf{n})$, where $\mathbf{n} = [n_x, n_y]^T$, and n_x and n_y are defined as vertical and horizontal indices in 2D signals. In the lifting structure of 1D DWT, the input signals are divided into even samples x_e and odd samples x_o as follows.

$$\begin{cases} x_e(\mathbf{n}) = x([n_x, 2n_y]^T) \\ x_o(\mathbf{n}) = x([n_x, 2n_y + 1]^T) \end{cases} \tag{9}$$

In the prediction step, odd samples $x_o(\mathbf{n})$ are predicted from the neighboring even samples $x_e(\mathbf{n})$ as

$$\hat{x}_o(\mathbf{n}) = x_o(\mathbf{n}) + p_e(\mathbf{n}), \tag{10}$$

where $p_e(\mathbf{n})$ is expressed as

$$p_e(\mathbf{n}) = p_i \left\{ x_e\left(\begin{bmatrix} n_x - \tan\theta_d \\ n_y \end{bmatrix} \right) + x_e\left(\begin{bmatrix} n_x + \tan\theta_d \\ n_y + 1 \end{bmatrix} \right) \right\},$$

p_i is a coefficient of filter and θ_d is arbitrary direction of filtering. Figure 4 shows $\theta_d = \{\pi/2, \pi/4, -\pi/4\}$. Next, in the update step, even samples $x_e(\mathbf{n})$ are updated from the new neighboring odd samples $\hat{x}_o(\mathbf{n})$ as

$$\hat{x}_e(\mathbf{n}) = x_e(\mathbf{n}) + u_o(\mathbf{n}), \tag{11}$$

where $u_o(\mathbf{n})$ is expressed as

$$u_o(\mathbf{n}) = u_i \left\{ \hat{x}_o\left(\begin{bmatrix} n_x - \tan\theta_d \\ n_y - 1 \end{bmatrix} \right) + \hat{x}_o\left(\begin{bmatrix} n_x + \tan\theta_d \\ n_y \end{bmatrix} \right) \right\},$$

u_i is a coefficient of filters. This set of lifting operations is repeated and conclusive samples are produced as lowpass and highpass coefficients.

3. Polyphase Representation of 2D Non-separable Lifting Structure of DWT

3.1 Generalized Structure

In this paper, we introduce the generalized polyphase representation of the 2D non-separable lifting structure of DWT. Here, some matrices are defined as follows.

$$\begin{aligned}
\mathbf{S} &= \mathrm{diag}\left(\begin{bmatrix} s & 0 \\ 0 & 1/s \end{bmatrix}, \begin{bmatrix} s & 0 \\ 0 & 1/s \end{bmatrix}\right), \quad \hat{\mathbf{S}} = \begin{bmatrix} s\mathbf{I} & \mathbf{0} \\ \mathbf{0} & 1/s\mathbf{I} \end{bmatrix}, \\
\mathbf{U}_i^j &= \mathrm{diag}\left(\begin{bmatrix} 1 & U_i^j \\ 0 & 1 \end{bmatrix}, \begin{bmatrix} 1 & U_i^j \\ 0 & 1 \end{bmatrix}\right), \quad \hat{\mathbf{U}}_i^j = \begin{bmatrix} \mathbf{I} & U_i^j\mathbf{I} \\ \mathbf{0} & \mathbf{I} \end{bmatrix}, \\
\mathbf{P}_i^j &= \mathrm{diag}\left(\begin{bmatrix} 1 & 0 \\ P_i^j & 1 \end{bmatrix}, \begin{bmatrix} 1 & 0 \\ P_i^j & 1 \end{bmatrix}\right), \quad \hat{\mathbf{P}}_i^j = \begin{bmatrix} \mathbf{I} & \mathbf{0} \\ P_i^j\mathbf{I} & \mathbf{I} \end{bmatrix}.
\end{aligned} \tag{12}$$

By using these matrices, (8) is rewritten as

$$\mathbf{E}(\mathbf{z}) = \mathbf{S} \prod_{i=N-1}^{0} \{\mathbf{U}_i^y \mathbf{P}_i^y\}\, \hat{\mathbf{S}} \prod_{i=N-1}^{0} \{\hat{\mathbf{U}}_i^x \hat{\mathbf{P}}_i^x\}. \tag{13}$$

Without a loss of generalities, the following relationships are satisfied.

$$\begin{cases} \mathbf{U}_i^y \mathbf{P}_i^y \hat{\mathbf{S}} = \hat{\mathbf{S}} \mathbf{U}_i^y \mathbf{P}_i^y, \\ \mathbf{U}_p^y \mathbf{P}_p^y \hat{\mathbf{U}}_q^x \hat{\mathbf{P}}_q^x = \hat{\mathbf{U}}_q^x \hat{\mathbf{P}}_q^x \mathbf{U}_p^y \mathbf{P}_p^y, \end{cases} \tag{14}$$

where $p, q = 0, 1, \ldots, N-1$. These relationships mean that some matrices can be moved, and (13) is rewritten as

$$\mathbf{E}(\mathbf{z}) = \mathbf{S}\hat{\mathbf{S}} \prod_{i=N-1}^{0} \{\mathbf{U}_i^y \mathbf{P}_i^y \hat{\mathbf{U}}_i^x \hat{\mathbf{P}}_i^x\}. \tag{15}$$

Some matrices are merged with each other and factorized into the non-separable structure. If $\mathbf{G}_{p,q}(\mathbf{z})$ is defined a product of matrices as

$$\mathbf{G}_{p,q}(\mathbf{z}) = \mathbf{U}_p^y \mathbf{P}_p^y \hat{\mathbf{U}}_q^x \hat{\mathbf{P}}_q^x, \tag{16}$$

where p and q are arbitrary integers, substituting (12) in (16), $\mathbf{G}_{p,q}(\mathbf{z})$ is consequently described as

$$\mathbf{G}_{p,q}(\mathbf{z}) = \begin{bmatrix} G_p^y G_q^x & U_p^y G_q^x & G_p^y U_q^x & U_p^y U_q^x \\ P_p^y G_q^x & G_q^x & P_p^y U_q^x & U_q^x \\ G_p^y P_q^x & U_p^y P_q^x & G_p^y & U_p^y \\ P_p^y P_q^x & P_q^x & P_p^y & 1 \end{bmatrix}, \tag{17}$$

where $G_k^j = 1 + P_k^j U_k^j$ (j : x or y, k : p or q). Consequently, $\mathbf{G}_{p,q}(\mathbf{z})$ can be factorized into a lifting structure as

$$\begin{aligned}
\mathbf{G}_{p,q}(\mathbf{z}) = &\begin{bmatrix} 1 & U_p^y & U_q^x & -U_p^y U_q^x \\ 0 & 1 & 0 & 0 \\ 0 & 0 & 1 & 0 \\ 0 & 0 & 0 & 1 \end{bmatrix} \begin{bmatrix} 1 & 0 & 0 & 0 \\ P_p^y & 1 & 0 & U_q^x \\ P_q^x & 0 & 1 & U_p^y \\ 0 & 0 & 0 & 1 \end{bmatrix} \\
&\times \begin{bmatrix} 1 & 0 & 0 & 0 \\ 0 & 1 & 0 & 0 \\ 0 & 0 & 1 & 0 \\ P_p^y P_q^x & P_q^x & P_p^y & 1 \end{bmatrix}.
\end{aligned} \tag{18}$$

This non-separating factorization achieves to reduce rounding operators through merging some matrices. Substituting (18) in (15), the generalized polyphase representation of 2D non-separable lifting structure of DWT is defined as

$$\mathbf{E}(\mathbf{z}) = \tilde{\mathbf{S}} \prod_{i=N-1}^{0} \mathbf{G}_{i,i}(\mathbf{z}), \tag{19}$$

where $\tilde{\mathbf{S}} = \mathbf{S}\hat{\mathbf{S}} = \mathrm{diag}(s^2, 1, 1, 1/s^2)$.

In this section, we propose the generalized polyphase representation of 2D non-separable lifting structure of DWT by using the relationships (14) and the non-separating factorization (18). We show some examples in the next section.

3.2 5/3 and 9/7 DWT

The generalized polyphase representation is proposed in the previous section. In this section, we present its examples based on 5/3 and 9/7 DWT. These DWTs are well known to be applied to the JPEG 2000.

From (19), the polyphase matrix of 2D non-separable lifting structure of 5/3 DWT is described as

$$\mathbf{E}(\mathbf{z}) = \mathbf{G}_{0,0}(\mathbf{z}). \tag{20}$$

On the other hand, in the case of 9/7 DWT, the polyphase matrix is factorized from (19), as

$$\mathbf{E}(\mathbf{z}) = \tilde{\mathbf{S}}\mathbf{G}_{1,1}(\mathbf{z})\mathbf{G}_{0,0}(\mathbf{z}). \tag{21}$$

However, the other polyphase matrix can be designed from the relationships (14) and the non-separating factorization (18). From (13) with $N = 2$, the other polyphase matrix is designed as

$$\begin{aligned}
\mathbf{E}(\mathbf{z}) &= \mathbf{S}\mathbf{U}_1^y \mathbf{P}_1^y \mathbf{U}_0^y \mathbf{P}_0^y \times \hat{\mathbf{S}}\hat{\mathbf{U}}_1^x \hat{\mathbf{P}}_1^x \hat{\mathbf{U}}_0^x \hat{\mathbf{P}}_0^x \\
&= \mathbf{S}\hat{\mathbf{S}} \times \mathbf{U}_1^y \mathbf{P}_1^y \times \mathbf{U}_0^y \mathbf{P}_0^y \hat{\mathbf{U}}_1^x \hat{\mathbf{P}}_1^x \times \hat{\mathbf{U}}_0^x \hat{\mathbf{P}}_0^x \\
&= \tilde{\mathbf{S}}\mathbf{U}_1^y \mathbf{P}_1^y \mathbf{G}_{0,1}(\mathbf{z}) \hat{\mathbf{U}}_0^x \hat{\mathbf{P}}_0^x.
\end{aligned} \tag{22}$$

This structure has been proposed in [14], and is shown in Fig. 5. Compared with Fig. 3, it is shown to require less rounding operators. Therefore, it is proven that the non-separable structure has better compatibilities to the conventional 9/7 DWTs in the JPEG 2000 than the separable structure [14]. In that sense, we design the polyphase matrix of 2D non-separable lifting structure of 9/7 DWT as (22).

4. 2D Non-separable ADL Structure of DWT

4.1 Realization

In this section, we propose the 2D non-separable ADL struc-

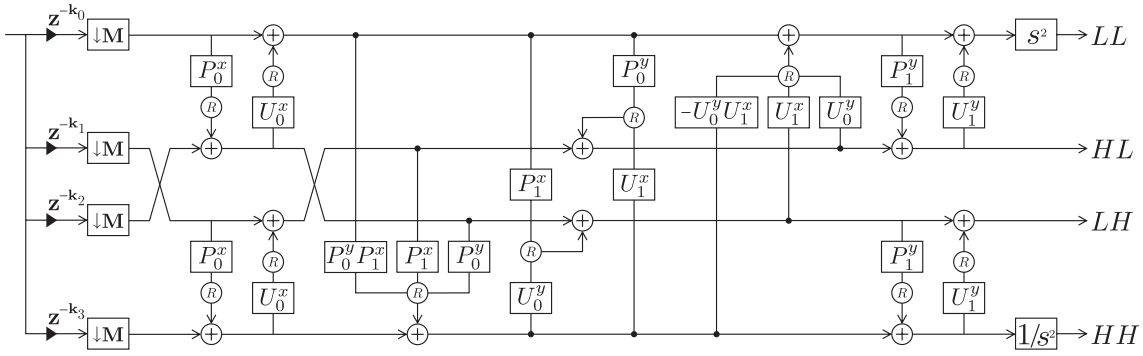

Fig. 5 2D non-separable lifting structure of 9/7 DWT.

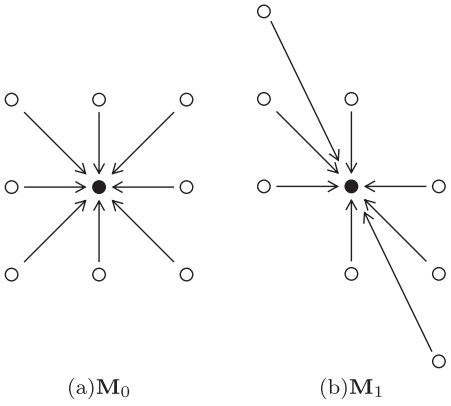

Fig. 6 Lifting direction of 2D ADL.

ture of DWT based on the 2D non-separable lifting structure of DWT shown in Sect. 3. The ADL structure can transform a sub-region of images along its direction. Therefore, the structure efficiently reduces the entropy of transformed coefficients and achieves better image coding performance.

By changing the sampling matrix $\mathbf{M}$ depending on sub-regions of images, the ADL structure is realized. Figure 6 shows one lifting operation, where these sampling matrices are defined as

$$\mathbf{M}_0 = \begin{bmatrix} 2 & 0 \\ 0 & 2 \end{bmatrix}, \ \mathbf{M}_1 = \begin{bmatrix} 2 & 2 \\ 0 & 2 \end{bmatrix}. \tag{23}$$

These dots are pixels, and black dots are transformed with neighbor white dots along arrows. This figure shows that neighbor pixels used for the lifting operation are changed by changing the sampling matrix in the sub-region. In other words, the direction of the transform can be changed by changing the sampling matrix.

The arbitrary sampling matrix whose absolute determinant is 4 can be selected. The following sampling matrices $\mathbf{M}_d$ ($d = 0, 1, \ldots, 6$) are used in this paper.

$$\mathbf{M}_d = \left\{ \begin{bmatrix} 2 & 0 \\ 0 & 2 \end{bmatrix}, \begin{bmatrix} 2 & 2 \\ 0 & 2 \end{bmatrix}, \begin{bmatrix} 2 & -2 \\ 0 & 2 \end{bmatrix}, \begin{bmatrix} 2 & 0 \\ 2 & 2 \end{bmatrix}, \begin{bmatrix} 2 & 0 \\ -2 & 2 \end{bmatrix}, \begin{bmatrix} 2 & 4 \\ 0 & 2 \end{bmatrix}, \begin{bmatrix} 2 & -4 \\ 0 & 2 \end{bmatrix} \right\}$$

With changing the sampling matrix, the delay vectors have to be changed. For maintaining the linear phase property of filters, we define the delay vectors to be symmetrical with respect to a point which is a center of $\mathbf{M}_d$. Table 1 shows the delay vectors corresponding to $\mathbf{M}_d$ and the directions of the transform are represented in Fig. 7. It shows that the proposed structure can transform along various directions besides vertical and horizontal shown in Fig. 7(a). Since 2D signals are transformed by $\mathbf{E}(\mathbf{z})$ after down-sampling with $\mathbf{M}_d$ and some delays, in this proposed structure, a sampling matrix can share the same transformed system produced by the polyphase matrix $\mathbf{E}(\mathbf{z})$ as the others.

Table 1 Delay vectors.

d	$\mathbf{k}_0$	$\mathbf{k}_1$	$\mathbf{k}_2$	$\mathbf{k}_3$
0	$[0,0]^T$	$[0,1]^T$	$[1,0]^T$	$[1,1]^T$
1	$[0,0]^T$	$[1,1]^T$	$[1,0]^T$	$[2,1]^T$
2	$[0,0]^T$	$[-1,1]^T$	$[1,0]^T$	$[0,1]^T$
3	$[0,0]^T$	$[0,1]^T$	$[1,1]^T$	$[1,2]^T$
4	$[0,0]^T$	$[0,1]^T$	$[1,-1]^T$	$[1,0]^T$
5	$[0,0]^T$	$[2,1]^T$	$[1,0]^T$	$[3,1]^T$
6	$[0,0]^T$	$[-2,1]^T$	$[1,0]^T$	$[-1,1]^T$

4.2 Optimal Direction Decision

For the image coding application, the optimal directions are decided according to the energy of highpass subband. Especially, we focus on the energy of HH subband in this paper. For all the sampling matrix $\mathbf{M}_d$, the HH subband components at a index $\mathbf{n}$ are described as $h_d(\mathbf{n})$. Practically, the directional information is assigned to not the pixels but the blocks divided by the quad tree decomposition in order to reduce the side information. For this purpose, R-D optimization is processed as in the following. The full quad tree T is constructed by applying the quad tree decomposition to the image until reaching the predefined block size. B, $D(B)$ and $R(B)$ are defined as an arbitrary subtree, a distortion and a rate of bits. The most suitable subtree B^* with optimal direction is provided by minimizing the cost function $J(B)$ expressed by

$$B^* = \min_B J(B) = \min_B (D(B) + \lambda R(B)), \tag{24}$$

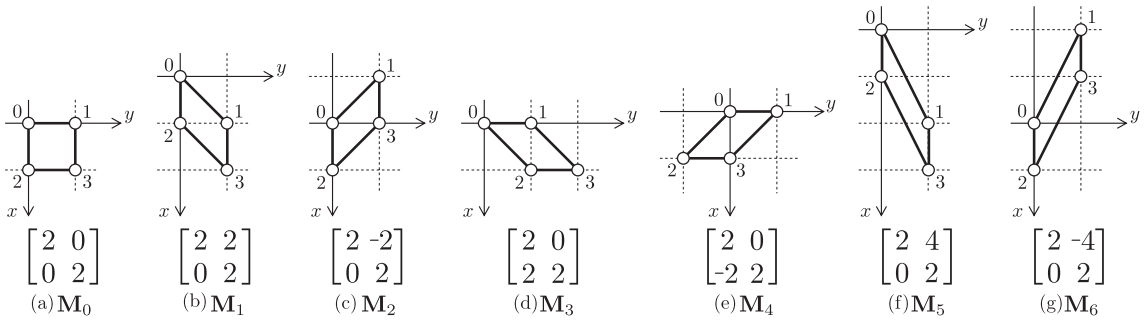

Fig. 7 Sampling matrices.

Table 2 Reduced numbers of computational costs.

	Direction decision		Image Transformation	
	5/3	9/7	5/3	9/7
Add.	$(1/2)DL$	$(3/2)DL$	$-2L$	L
Mult.	$(1/2)DT$	$(5/4)DL$	$(-1/2)L$	$(7/4)L$
Round.	DL	$2DL$	L	$(17/4)L$

where

$$D(B) = \sum_{\tau \in B} \sum_{\mathbf{n} \in N_\tau} |h_{\tau,d}(\mathbf{n})|^2,$$
$$R(B) = \sum_{\tau \in B} r_C(\tau) + \sum_{v \in B} r_T(v),$$

τ denotes a node of B, N_τ is a support region in images at a node τ, $|h_{\tau,d}(\mathbf{n})|$ is $|h_d(\mathbf{n})|$ at a node τ, $r_C(\tau)$ and $r_T(v)$ are defined as the rate of the entropy encoding highpass coefficients in τ and coding the side information in node in v, respectively.

4.3 Comparison of Computational Costs

In Table 2, we show the differences of the computational costs between the 1D ADL structure and the proposed 2D ADL of 5/3 and 9/7 DWTs by subtracting 2D ADL from 1D ADL. "Add.", "Mult.", "Round.", "5/3" and "9/7" mean addition, multiplication, rounding, 5/3 DWT and 9/7 DWT, respectively. These numbers depend on the size L of input images and their lifting steps. Additionally, the numbers D of direction candidates for lifting should be taken into account for the lifting direction decision.

Table 2 shows that the proposed structure is simpler than the 1D ADL in terms of the computational costs. For the adaptive directional filtering, we need at least three directions which are vertical or horizontal, diagonal from top left to bottom right, and diagonal from top right to bottom left. Hence, by substituting $D = 3$ and adding the numbers of the directional decision and image transformation, total numbers of the reduced addition and multiplication are $(-1/2)L$ and L, in the case of the 5/3 DWT. The multiplication has more loads in the computation and implementation than the addition. Therefore, the both proposed structures are considered to be simpler than the 1D ADL structures.

5. Simulation

We apply the proposed ADL structure of 5/3 and 9/7 DWTs into the lossy and lossless image coding application and compare the coding efficiency with the conventional structure of 5/3 and 9/7 DWTs.

For the comparisons, we use the 2D separable lifting structure of DWT in (8), the 2D non-separable lifting structure of DWT in (20), and the 1D ADL structure of DWT shown in Sect. 2.3. In this section, for simple notations, these conventional structures and the proposed structure are denoted as 1D DWT, 2D DWT, 1D ADL and 2D ADL, respectively. The 1D and 2D DWTs are applied to images with 6-level octave decomposition. In cases of the 1D and 2D ADLs, the 1D and 2D DWTs are applied to images at the second to sixth levels after the 1D and 2D ADL structures of DWT are applied at only the first level, respectively[†].

For reducing the side information and computational costs, the candidate directions are restricted three and seven in the 5/3 and 9/7 DWTs, respectively. There exists a tradeoff between better compression rate and less computational costs. These restrictions are experimentally decided for the valid comparison.

The embedded zerotree wavelet based on intraband partitioning (EZW-IP) [15] is used as the encoder. Since transformed coefficients are integer and encoded images are lossless bit streams, lossy bit streams are produced by discarding the backward bits of the bit streams. The side information is encoded by the arithmetic coding algorithm [16]. At the lossy image coding application, the peak signal-to-noise ratio (PSNR) is used as an objective function measuring an image quality of reconstructed images. The PSNR is formulated as

$$\mathrm{PSNR} = 10 \log_{10} \frac{255^2}{\mathrm{MSE}}, \tag{25}$$

where MSE means the mean square error.

[†]The 1D ADL is applied at an only vertical direction in the first level for fairy comparison. In that case, the number of side information bits is equal to case of the 2D ADL.

Table 3 Image coding results of 5/3 DWT [bpp].

	1D DWT	2D DWT	1D ADL	2D ADL
Zone plate	6.78	6.78	6.73	6.12
Barbara	4.87	4.86	4.84	4.78
Lena	4.50	4.49	4.49	4.48

5.1 5/3 DWT for Lossless

The 2D non-separable ADL structure of 5/3 DWT is applied into the lossless image coding. The 2D ADL is realized by imposing the directional selectivity on the 2D non-separable lifting structure of 5/3 DWT described in (20), as shown in Sect. 4. For reducing the side information, the selected directions are experientially-restricted to be three in this paper. θ_d in Sect. 2.3 is selected as $\{\pi/2, \pi/4, -\pi/4\}$ in the 1D ADL structure of DWT, and $\mathbf{M}_d$ $(d = 0, 1, 2)$ is selected in the 2D ADL. They are not correctly same directions due to the down-sampling, but considered to be a reasonable comparison.

Table 3 indicates results of the lossless image coding application. These values are entropies of compressed images described in bit-per-pixel (bpp), and the entropy of 1D ADL and 2D ADL includes the encoded side information. In the case of *Zone plate* and *Barbara*, the 2D ADL is efficient for images having rich directional components because of the small number of rounding operators and the adaptive directional filtering. On the other hand, the proposed structure is slightly effective for images whose energy is concentrated on the low frequency region such as *Lena*.

5.2 9/7 DWT for Lossy-to-Lossless

In a similar way to the 5/3 DWT, the 2D ADL structure of 9/7 DWT is applied into the lossy and lossless image coding. The 2D ADL is based on (22), with $\mathbf{M}_d$ $(d = 0, 1, \cdots, 6)$, and $\tan\theta_d = \{0, 1, -1, 2, -2, 0.5, -0.5\}$ in the 1D ADL.

Table 4 indicates results of the lossy and lossless image coding application. In the lossy, these numbers are PSNR of reconstructed images in dB, and rates are described in bpp. The proposed structure improves image coding application in the lossy and lossless for the same reason of 5/3 DWT. Compared with the 1D and 2D DWTs, the 2D ADL shows more efficient image coding results because of fewer rounding operations and adaptive directional filtering. However, the adaptive directional filtering is considered to be slightly effective for some images such as *Lena* due to the same reason as the 5/3 DWT, as in the discussion in Sect. 5.1. On the other hand, compared with 1D ADL, some coding results of the 2D ADL show worse performance because the 1D and 2D ADLs are not in a same class of the adaptive directional filtering. However, it is an advantage that the structure of the 2D ADL is the simpler than one of the 1D ADL. In this methods, the image coding performance depends on the decided directions for sub-regions. In a future work, there exists a better optimal directional decision for the 2D ADL.

Table 4 Image coding results of 9/7 DWT.

Lossless [bpp]				
	1D DWT	2D DWT	1D ADL	2D ADL
Zone plate	6.11	6.08	4.93	5.33
Barbara	4.84	4.81	4.81	4.75
Lena	4.54	4.51	4.54	4.51

Lossy [dB]					
	Rate	1D DWT	2D DWT	1D ADL	2D ADL
Zone plate	0.25	12.01	12.02	13.32	13.48
	0.5	15.19	15.19	17.91	17.50
	1	19.98	19.98	24.56	22.94
Barbara	0.25	27.24	27.23	27.43	27.60
	0.5	30.46	30.45	30.82	30.94
	1	34.85	34.84	35.14	35.28
Lena	0.25	32.52	32.50	32.54	32.54
	0.5	35.52	35.48	35.60	35.52
	1	38.39	38.34	38.44	38.38

Fig. 8 Original images and reconstructed images.

In Fig. 8, the original and reconstructed images are represented, where the compression rate is 0.25 [bpp]. Compared with the conventional structure which does not have an adaptive directional selectivity, the proposed structure can represent various directions besides vertical and horizontal. Especially, stripe textures in Fig. 8(f) are represented clearly.

6. Conclusion

In this paper, we generalize the polyphase representation of the 2D non-separable lifting structure of DWT and propose ADL of the structure. With maintaining the advantage of the 2D non-separable and the adaptive directional filtering, the proposed structure achieves efficient image coding results.

Acknowledgments

This work was supported by Global COE Program "High-Level Global Cooperation for Leading-Edge Platform on Access Spaces (C12)".

References

[1] ISO/IEC 10918-1, Information technology — JPEG 2000 image coding system: Core coding system.
[2] A. Descampe, F.O. Devaux, G. Rouvroy, J.D. Legat, J.J. Quisquater, and B. Macq, "A flexible hardware JPEG 2000 decoder for digital cinema," IEEE Trans. Circuits Syst. Video Technol., vol.16, no.11, pp.1397–1410, Nov. 2006.
[3] Ömer N. Gerek and A.E. Çetin, "A 2-D orientation-adaptive prediction filter in lifting structures for image coding," IEEE Trans. Image Process., vol.15, no.1, pp.106–111, Jan. 2006.
[4] C.L. Chang and B. Girod, "Direction-adaptive discrete wavelet transform for image compression," IEEE Trans. Image Process., vol.16, no.5, pp.1289–1302, May 2007.
[5] W. Ding, F. Wu, X. Wu, S. Li, and H. Li, "Adaptive directional lifting-based wavelet transform for image coding," IEEE Trans. Image Process., vol.16, no.2, pp.416–427, Feb. 2007.
[6] W. Dong, G. Shi, and J. Xu, "Adaptive nonseparable interpolation for image compression with directional wavelet transform," IEEE Signal Process. Lett., vol.15, no.1, pp.233–236, 2008.
[7] Y. Liu and K.N. Ngan, "Weighted adaptive lifting-based wavelet transform for image coding," IEEE Trans. Image Process., vol.17, no.4, pp.500–511, April 2008.
[8] G. Quellec, M. Lamard, G. Cazuguel, B. Cochener, and C. Roux, "Adaptive nonseparable wavelet transform via lifting and its application to content-based image retrieval," IEEE Trans. Image Process., vol.19, no.1, pp.25–35, Jan. 2010.
[9] Y. Tanaka, M. Hasegawa, S. Kato, M. Ikehara, and T.Q. Nguyen, "Adaptive directional wavelet transform based on directional prefiltering," IEEE Trans. Image Process., vol.19, no.4, pp.934–945, April 2010.
[10] I. Daubechies and W. Sweldens, "Factoring wavelet transforms into lifting steps," J. Fourier Anal. Appl., vol.4, no.3, pp.247–269, 1998.
[11] M. Iwahashi, "Four-band decomposition module with minimum rounding operations," IET Electronics Lett., vol.43, no.6, pp.27–28, March 2007.
[12] M. Iwahashi and H. Kiya, "Reversible 9–7 DWT compatible to irreversible 9–7 DWT of JPEG 2000," IEICE Techical Report, IE2008-257, March 2009.
[13] P.P. Vaidyanathan, Multirate Systems and Filter Banks, Prentice-Hall, Englewood Cliffs, NJ, 1993.
[14] M. Iwahashi and H. Kiya, "Non separable 2D factorization of separable 2D DWT for lossless image coding," IEEE ICIP'09, pp.17–20, Nov. 2009.
[15] Z. Liu and L.J. Karam, "An efficient embedded zerotree wavelet image codec based on intraband partitioning," IEEE ICIP'00, pp.162–165, Sept. 2000.
[16] P.G. Howard and J.S. Vitter, "Arithmetic coding for data compression," Proc. IEEE, vol.82, no.6, pp.857–865, June 1994.

Taichi Yoshida received the B.E. and M.E. degrees in electrical engineering from Keio University, Yokohama, Japan, in 2006 and 2008, respectively. He is currently a Ph.D. candidate at Keio University, Yokohama, Japan, under the supervision of Prof. Masaaki Ikehara. His research interests are in the field of filter bank design and its image coding application.

Taizo Suzuki received the B.E., M.E. and Ph.D. degrees in electrical engineering from Keio University, Yokohama, Japan, in 2004, 2006 and 2010, respectively. He joined Toppan Printing Co., Ltd., Tokyo, Japan, from 2006 to 2008. From 2008 to 2011, he was a Research Assistant (RA) of Global Center of Excellence (G-COE) at Keio University. Also, he was a Research Fellow of the Japan Society for the Promotion of Science (JSPS) from 2010 to 2011. Moreover, he was a Visiting Scholar at the University of California, San Diego (Video Processing Group supervised by Prof. T. Q. Nguyen) from 2010 to 2011. He is currently an Assistant Professor at College of Engineering, Nihon University. His current research interests are M-channel filter bank design and its application for image/video signal processing.

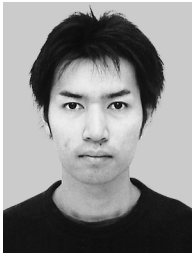

Seisuke Kyochi received the B.S. degree in mathematics from Rikkyo University, Toshima, Japan in 2005 and the M.E. and Ph.D. degrees from Keio University, Yokohama, Japan in 2007 and 2010, respectively. He is currently with the Video Coding Group of NTT Cyber Space Laboratories. His research interests in the areas of wavelets, filter banks and their application to image and video coding.

Masaaki Ikehara received the B.E., M.E. and Dr.Eng. degrees in electrical engineering from Keio University, Yokohama, Japan, in 1984, 1986, and 1989, respectively. He was Appointed Lecturer at Nagasaki University, Nagasaki, Japan, from 1989 to 1992. In 1992, he joined the Faculty of Engineering, Keio University. From 1996 to 1998, he was a visiting researcher at the University of Wisconsin, Madison, and Boston University, Boston, MA. He is currently a Full Professor with the Department of Electronics and Electrical Engineering, Keio University. His research interests are in the areas of multirate signal processing, wavelet image coding, and filter design problems.